



HAL
open science

Crustacean cardioactive peptides Expression, localization, structure, and a possible involvement in regulation of egg-laying in the cuttlefish *Sepia officinalis*

Maxime Endress, Céline Zatylny-Gaudin, Erwan Corre, Gildas Le Corguille, Louis Benoist, Jérôme Leprince, Benjamin Lefranc, Benoît Bernay, Alexandre Leduc, Jimmy Rangama, et al.

► To cite this version:

Maxime Endress, Céline Zatylny-Gaudin, Erwan Corre, Gildas Le Corguille, Louis Benoist, et al.. Crustacean cardioactive peptides Expression, localization, structure, and a possible involvement in regulation of egg-laying in the cuttlefish *Sepia officinalis*. *General and Comparative Endocrinology*, 2018, 260, pp.67-79. 10.1016/j.ygcen.2017.12.009 . hal-01744294

HAL Id: hal-01744294

<https://univ-rennes.hal.science/hal-01744294>

Submitted on 4 Apr 2018

HAL is a multi-disciplinary open access archive for the deposit and dissemination of scientific research documents, whether they are published or not. The documents may come from teaching and research institutions in France or abroad, or from public or private research centers.

L'archive ouverte pluridisciplinaire **HAL**, est destinée au dépôt et à la diffusion de documents scientifiques de niveau recherche, publiés ou non, émanant des établissements d'enseignement et de recherche français ou étrangers, des laboratoires publics ou privés.

Title: Crustacean cardioactive peptides: expression, localization, structure, and a possible involvement in regulation of egg-laying in the cuttlefish *Sepia officinalis*

Authors: Maxime Endress¹, Céline Zatylny-Gaudin¹, Erwan Corre³, Gildas Le Corguillé³, Louis Benoist¹, Jérôme Leprince⁴, Benjamin Lefranc⁴, Benoît Bernay⁶, Alexandre Leduc¹, Jimmy Rangama⁶, Anne-Gaëlle Lafont⁵, Arnaud Bondon⁵, Joël Henry^{1,5}

1: Normandy University, UNICAEN, Sorbonne Universités, MNHN, UPMC Univ Paris 06, UA, CNRS, IRD, Biologie des Organismes et Ecosystèmes Aquatiques (BOREA), F-14032 Caen, France.

2: UPMC, CNRS, FR2424, ABiMS, Station Biologique, F-29680 Roscoff, France.

3: Normandy University, UNIROUEN, INSERM, U1239, Laboratoire Différenciation et Communication Neuronale et Neuroendocrine, Institut de Recherche et d'Innovation Biomédicale de Normandie, F-76000 Rouen, France.

4: Equipe CORINT, UMR CNRS 6226, PRISM, CS 34317, Campus de Villejean, Université de Rennes 1, F-35043 Rennes, France.

5: Normandy University, Post Genomic Platform PROTEOGEN, SF ICORE 4206, F-14032 Caen, France.

6: Normandy University, CIMAP, UMP 6252 (CEA/CNRS/ENSICAEN/Normandy University), Caen, France.

Corresponding author: Joël HENRY. joel.henry@unicaen.fr

Address: Normandy University, UMR BOREA, Esplanade de la paix, F-14000 Caen, France.

Abstract

The cuttlefish (*Sepia officinalis*) is a cephalopod mollusk distributed on the western European coast, in the West African Ocean and in the Mediterranean Sea. On the Normandy coast (France), cuttlefish is a target species of professional fishermen, so its reproduction strategy is of particular interest in the context of stock management. Egg-laying, which is coastal, is controlled by several types of regulators among which neuropeptides. The cuttlefish neuropeptidome was recently identified by Zatylny-Gaudin et al. (2016). Among the 38 neuropeptide families identified, some were significantly overexpressed in egg-laying females as compared to mature males.

This study is focused on crustacean cardioactive peptides (CCAPs), a highly expressed neuropeptide family strongly suspected of being involved in the control of egg-laying. We investigated the functional and structural characterization and tissue mapping of CCAPs, as well as the expression patterns of their receptors. CCAPs appeared to be involved in oocyte transport through the oviduct and in mechanical secretion of capsular products. Immunocytochemistry revealed that the neuropeptides were localized throughout the central nervous system (CNS) and in the nerve endings of the glands involved in egg-capsule synthesis and secretion, i.e. the oviduct gland and the main nidamental glands. The CCAP

receptor was expressed in these glands and in the subesophageal mass of the CNS. Multiple sequence alignments revealed a high level of conservation of CCAP protein precursors in *Sepia officinalis* and *Loligo pealei*, two cephalopod decapods. Primary sequences of CCAPs from the two species were fully conserved, and cryptic peptides detected in the nerve endings were also partially conserved, suggesting biological activity that remains unknown for the time being.

Keywords: neuropeptides, CCAPs, egg-laying, NMR, *Sepia officinalis*, Cephalopod

Abbreviations: ACN: acetonitrile; CCAPs: crustacean cardioactive peptides; CNS: central nervous system; DTT: dithiothreitol; ELH: egg-laying hormone; FPKM: fragments per kilobase of exon per million fragments mapped; MNG: main nidamental gland; NMR: nuclear magnetic resonance; OvG: oviduct gland; SoCCAPs: *Sepia officinalis* CCAPs; SubEM: subesophageal mass; SupEM: supraesophageal mass; TFA: trifluoroacetic acid.

1. Introduction

In the cuttlefish *Sepia officinalis*, spawning begins with the release of mature oocytes into the genital coeloma, followed by their retention until mating. This blockage prevents oocyte emission if the female cuttlefish has not been fertilized. Mating triggers peristaltic contractions of the oviduct that restart oocyte transport through the genital tract. A first inner layer of the capsule is secreted by the oviduct gland (OvG), which is closely associated with the distal oviduct. The partially encapsulated oocyte is released into the mantle cavity where the outer capsule is secreted by the main nidamental glands (MNGs). This second capsule is made of egg-capsule proteins (Cornet et al., 2015) which make up a network with polysaccharides, bacteria, and melanin from the ink bag. The encapsulated oocyte quits the mantle cavity through the siphon, probably carried by the gill-current associated with siphon contractions, and remains approximately 3 minutes in a cavity formed by the arms and the buccal mass. At this stage, fertilization takes place with the spermatozoa stored by the female since mating. The eggs are finally laid on a supporting material near the bottom, e.g. seaweeds, to form the egg mass. The successive ovulation, oocyte transport, encapsulation and fertilization steps are orchestrated by neuropeptides (Henry et al., 2013, 1999, 1997), ovarian regulatory peptides (Bernay et al., 2006, 2005, 2004, Zatylny et al., 2000a, 2000b), and sex pheromones (Enault et al., 2012).

Although neuropeptides are not the only regulators involved in regulation of egg-laying mechanisms, they nevertheless play an important role in integrating environmental parameters such as the photoperiod, temperature, salinity or depth. Expressed and released by neurons, they make up a highly diversified category by their structure, their mode of action, and the physiological functions they regulate.

In cuttlefish, neuropeptides like APGWamide (Henry et al., 1997), FMRFamide (Henry et al., 1999) and sepiatocin (Henry et al., 2013) play a role in oocyte transport and capsular secretion. In other mollusks such as the Sydney Rock Oyster (*Saccostrea glomerata*), several neuropeptides induce egg laying in sexually mature individuals: egg-laying hormone (ELH), GnRH, APGWamide, buccalin, CCAPs (crustacean cardioactive peptides), and LFRFamide (In et al., 2016). In gastropods, ELH appears to be pivotal in egg-laying regulation, particularly in hermaphrodite snails such as *Aplysia* (Arch, 1972; Chiu et al., 1979; Chiu and Strumwasser, 1981) and *Lymnaea* (Ebberink et al., 1985; Geraerts et al., 1983; Vreugdenhil et al., 1985), whereas in gonochoric gastropods many neuropeptides also appear to be involved in addition to ELH. In the abalone *Haliotis asinina*, several genes encoding APGWamide, myomodulin, proctolin-like, FMRFamide, schistosomin-like, insulin and a halotid growth-

associated peptide are differentially expressed during the two-week spawning cycle in both male and female abalone (York et al., 2012).

A recent study in cuttlefish (*S. officinalis*) identified the neuropeptidome as composed of at least 38 distinct families (Zatylny-Gaudin et al., 2016). On the basis of expression patterns and tissue localization, several neuropeptide families were strongly suspected to be involved in the control of the successive steps that lead to the formation and release of encapsulated eggs: APGWamide, CCAPs, clonin, FLGamide, PTSP-like peptides, SCP (small cardioactive peptide), insulin, myomodulin, sepiatocin and SPamide.

The present study is focused on *SoCCAPs* (for *Sepia officinalis* CCAPs), which are highly overexpressed in egg-laying females *versus* mature males and are detected by mass spectrometry in the nerve endings of mature female OvG.

The first CCAP was initially identified in *Carcinus maenas* on the basis of its cardioresponsive activity (Stangier et al., 1987). Later, the same peptide was found to modulate oviduct activity in *Locusta migratoria* (Donini et al., 2001) and therefore thought to be involved in egg emission. Furthermore, this neuropeptide is also involved in fertilization in *L. migratoria* since it increases the basal tonus and the frequency of spontaneous spermatheca contractions (da Silva and Lange, 2006).

In *C. maenas*, the CCAP protein precursor (Figure 1A) encodes one copy of a single neuropeptide: PFCNAFTGCamide (Chung et al., 2006), also found in many arthropods such as *Drosophila melanogaster* (Adams et al., 2000), *Manduca sexta* (Loi et al., 2001), *Periplaneta americana* (Honegger et al., 2002), *Euphausia crystallorophias* (Toullec et al., 2013), *Homarus americanus* (Christie et al., 2017), and *Chorismus antarcticus* (Toullec et al., 2017). From a structural point of view, analysis of the *S. officinalis* precursor predicted the release of 3 neuropeptides with very similar sequences, subsequently characterized by mass spectrometry (Zatylny-Gaudin et al., 2016). A special feature of these neuropeptides lies in the fact that although they are not amidated at their C-terminal end they keep the characteristic disulfide bond, in contrast to CCAPs from arthropods and bivalves (In et al., 2016). We named these neuropeptides based on the order of their occurrence in the precursor: *SoCCAP1* (VFCNSFGGCTNI), *SoCCAP2* (VFCNSYGGCKSF), and *SoCCAP3* (VFCNSFGGQON). The neuropeptidome of the gastropod *Deroceras reticulatum* recently revealed 2 precursors able to release 3 CCAPs each, including one non-amidated peptide (Ahn et al., 2017). In other gastropods like *Lottia gigantea* (Veenstra, 2010) or *Aplysia californica* (XP_005103388.1), 3 amidated CCAPs are predicted to be generated from their precursor (Figure 1B). In addition, as observed in arthropods, the primary sequence of molluscan CCAPs is well conserved (Figure 1B), suggesting a major physiological role. In arthropods, a phylum with abundant physiological data, the involvement of CCAPs is well described in many main regulation pathways controlling the heart rate, ecdysis behavior, or oviduct contraction in insects such as *Manduca sexta* (Lehman et al., 1993), *Tenebrio molitor* (Furuya et al., 1993), *D. melanogaster* (Baker et al., 1999; Dulcis et al., 2005; Dulcis and Levine, 2003), *L. migratoria* (Donini et al., 2001), *Anopheles gambiae* (Estévez-Lao et al., 2013), or in crustaceans such as *C. maenas* (Stangier et al., 1987) and *Cancer magister* (McGaw et al., 1995).

The aim of the present study was to demonstrate the involvement of *SoCCAPs* in the regulation mechanisms of egg-laying in cuttlefish (*S. officinalis*). In this perspective, we investigated tissue expression of *SoCCAPs* and their putative receptor. The neuropeptides were localized by immunostaining using specific polyclonal antibodies, and characterized by mass spectrometry. The capacity of *SoCCAPs* to adopt a defined structure in a membrane mimicking their environment was evaluated by nuclear magnetic resonance (NMR). Biological activity was assessed by a myotropic bioassay performed on the ovarian stroma (oocyte release into the genital coelom), the distal oviduct (oocyte release into the mantle

cavity and internal egg capsule secretion), and the MNGs outer egg-capsule secretion). Finally, expression of the receptor was studied in the different tissues by an *in silico* approach from the transcriptomes produced by Zatylny-Gaudin et al. (2016).

2. Materials and methods

2.1 Animal and tissue collection

All mature cuttlefish were trapped in the Bay of Seine between April and June 2015, 2016 and 2017. They were maintained in 1,000-liter outflow tanks at $15 \pm 1^\circ\text{C}$ at the Marine Station of Luc-sur-Mer (University of Caen-Normandy, France) under a natural photoperiod. Organs were dissected on animals anesthetized with 3% ethanol according to (Gonçalves et al., 2012), and then immediately frozen in liquid nitrogen or stored in artificial seawater (Reef crystal®) containing 1 mM glucose and maintained at 18°C , or fixed in Davidson solution. All applicable guidelines for care and use of animals were followed. Procedures were approved by the regional ethical committee (Comité d'Éthique Normandie en Matière d'Expérimentation Animale, CENOMEXA; agreement number 54).

2.2 Expression data

Transcriptome sequencing, assembly and annotation are described in Zatylny-Gaudin et al. (2016). Expression was quantified using fragments per kilobase of exon per million fragments mapped (FPKM) values from the 16 tissue-specific transcriptomes. The FPKM values of a given transcript from several tissues were compared to establish an expression pattern. In this case, FPKM values represented the pooled expression of five animals used to determine each transcriptome.

2.3 Sequence alignment and comparison

Multiple sequence alignments of CCAPs, CCAP precursors and putative CCAP G-protein-coupled receptors from mollusks and arthropods were performed using CLC Main Workbench 6.7.1 and SIM - Alignment Tool for protein sequences (Expasy). Transmembrane domains of cephalopod GPCRs were predicted with the web tools HMMTOP (<http://www.enzim.hu/hmmtop/index.php>), TMHMM version 2.0 (<http://www.cbs.dtu.dk/services/TMHMM/>) and I-TASSER (<https://zhanglab.cmb.med.umich.edu/I-TASSER/>), and finally aligned with the CCAP GPCR of *Apis mellifera* for which transmembrane domains were predicted by multiple sequence alignments (Garcia et al., 2015).

2.4 Tissue mapping by mass spectrometry

2.4.1 Peptide extraction

Each tissue extraction was performed from 3 animals. Tissues were crushed in liquid nitrogen and extracted for 30 minutes in the extraction buffer containing cold methanol/water/acetic acid (90/9/1) adjusted to 50 mM dithiothreitol (DTT). One gram of tissue was used for 10 mL of extraction buffer. The extract was centrifuged 20 min at $20,000 \times g$ at 4°C , and then the supernatant was evaporated in a speed vac. Dry pellets were resuspended in 0.1% trifluoroacetic acid (TFA), concentrated on C18 Sep-Pak cartridges (360 mg, Waters) and eluted with 80% acetonitrile (ACN) in water adjusted to 0.1% TFA.

2.4.2 NanoLC-MALDI-TOF/TOF analysis

2.4.2.1 Sample preparation for mass spectrometry analysis

Concentrated and desalted pellets were reduced with 100 mM DTT at 55°C for 60 min, alkylated with 50 mM iodoacetamide at 55°C for 45 min, and then re-concentrated and desalted on C18 OMIX-tips (10 µL, AGILENT). The chromatography step was performed on a nano-LC system (Prominence, Shimadzu). Peptides were concentrated on a Zorbax 5x0.3mm C18 precolumn (Agilent), and separated on a Zorbax 150x75µm C18 column (Agilent). Mobile phases consisted of 0.1% TFA in 99.9% water (v/v) (A) and 0.1% TFA in 99.9% ACN (v/v) (B). The nanoflow rate was set at 300 nL/min, and the gradient profile was as follows: constant 2% B for 5 min, from 2 to 5% B in 1 min, from 5 to 32% B in 144 min, from 32 to 70% B in 10 min, from 70 to 90% B in 5 min, and back to 2% B in 10 min. The 300 nL/min volume of the peptide solution was mixed with 1.2 µL/min volumes of solutions of 5 mg/mL of an α -cyano-4-hydroxycinnamic acid (CHCA) matrix prepared in a diluent solution of 50% ACN containing 0.1% TFA. Twenty-second fractions were spotted by an AccuSpot spotter (Shimadzu) on stainless steel Opti-TOF™ 384 targets.

2.4.2.2 Mass spectrometry analysis

MS experiments were carried out on an AB Sciex 5800 proteomics analyzer equipped with TOF TOF ion optics and OptiBeam™ on-axis laser irradiation with 1,000 Hz repetition rate. The system was calibrated before analysis with a mixture of des-Arg-bradykinin, angiotensin I, Glu1-fibrinopeptide B, ACTH (18-39) and ACTH (7-38), and mass precision was better than 50 ppm in reflectron mode. A laser intensity of 3400 was typically employed for ionizing. MS spectra were acquired in the positive reflector mode by summarizing 1,000 single spectra (5 × 200) in the 700 to 4,000 Da mass range. MS/MS spectra from the twenty most intense ions were acquired in the positive MS/MS reflector mode by summarizing a maximum of 2,500 single spectra (10 × 250) with a laser intensity of 4300. For tandem MS experiments, the acceleration voltage was 1 kV, and air was used as the collision gas. Gas pressure medium was selected as settings.

2.4.2.3 Peptide sequencing and protein precursor identification

The fragmentation pattern based on the occurrence of y, b and a ions was used to determine peptide sequences. Database searching was performed using the Mascot 2.5.1 program (Matrix Science). A database corresponding to a homemade *S. officinalis* transcript database (including 356,644 entries) was used (BioProject PRJNA242869). The variable modifications allowed were as follows: methionine oxidation and dioxidation, C-terminal amidation, and N-terminal pyroglutamate. “No enzyme” was selected. Mass accuracy was set to 200 ppm and 0.6 Da for the MS and MS/MS modes, respectively.

2.5 Immunolocalization of CCAPs

The central nervous system (CNS), the distal end of the oviduct, the OVG and MNGs were freshly dissected from n=3 animals and placed in a modified Davidson's fixative solution (30% sea filtered water, 30% ethanol 95%, 20% formalin 37%, 10% glycerol, 10% acetic acid for 24 to 48 h, at 4°C. Tissues were dehydrated in several baths containing increasing ethanol contents. Tissues were completely dehydrated by a bath of butanol before paraffin inclusion. 5-µm sections were deparaffined with Roti®-Histol (Carl Roth®), and incubated in H₂O₂-methanol 3% for 10 minutes at room temperature. Rehydration was performed in several baths of decreasing ethanol contents, Tris buffer (Tris-HCl 100 mM, pH 7.4), and TT buffer (Tris buffer, 0.5% TritonX-100). Neutralization of non-specific sites was performed by incubation in bovine serum albumin (BSA) 3% in TT buffer. Diluted (1:500 or 1:1,000) *SoCCAP* antibodies (Rabbit, GeneCust®, directed against *SoCCAP1*) in TT buffer were applied on the sections and incubated overnight at 4°C. Conjugated anti-rabbit antibody peroxidase diluted 1:500 in TT buffer (Invitrogen™ A16029) was applied on the sections and

incubated 1 hour at room temperature. Cells and nervous fibers containing immunolabelled material were visualized using diaminobenzidine (SIGMAFAST™ 3,3'-Diaminobenzidine tablets) as a chromogen. Slides were finally counterstained with hematoxylin for 30 seconds. The primary antibody was preabsorbed with 20 µg/mL of antigen as a pre-absorption control for specificity. Alternatively, the primary antibody was omitted.

2.6 Neuropeptide synthesis

2.6.1 Chemicals and reagents

Fmoc-L-amino acid residues were purchased from Iris Biotech (Marktredwitz, Germany). Preloaded polyethylene glycol-polystyrene resins (Fmoc-Asn(Trt)-PEG-PS, Fmoc-Ile-PEG-PS and Fmoc-Phe-PEG-PS) and *O*-benzotriazol-1-yl-*N,N,N',N'*-tetramethyluronium hexafluorophosphate (HBTU) were purchased from Life Technologies (Villebon-sur-Yvette, France). ACN, dimethylformamide (DMF) and *N*-methylpyrrolidone (NMP) were purchased from Biosolve Chimie (Dieuze, France). Diisopropylethylamine (DIEA), piperidine, anisole, TFA, thallium(III) trifluoroacetate (Tl(CF₃COO)₃) and other reagents were purchased from Sigma-Aldrich (Saint-Quentin-Fallavier, France).

2.6.2 Peptide synthesis

SoCCAP1 (H-Val-Phe-Cys-Asn-Ser-Phe-Gly-Gly-Cys-Thr-Asn-Ile-OH; LV-5347), *SoCCAP2* (H-Val-Phe-Cys-Asn-Ser-Tyr-Gly-Gly-Cys-Lys-Ser-Phe-OH; LV-5348), and *SoCCAP3* (H-Val-Phe-Cys-Asn-Ser-Phe-Gly-Gly-Cys-Gln-Asn-OH; LV-5346) were synthesized (0.1 mmol scale) on Fmoc-Ile-PEG-PS, Fmoc-Phe-PEG-PS or Fmoc-Asn(Trt)-PEG-PS resins, respectively, using an Applied Biosystems model 433A automatic peptide synthesizer and the standard procedures, as previously described (Chatenet et al., 2006; Quan et al., 2015). All Fmoc-amino acids (1 mmol, 10 eq.) were coupled by *in situ* activation with HBTU (1.25 mmol, 12.5 eq.) and DIEA (2.5 mmol, 25 eq.) in NMP. Reactive side-chains were protected as follows: Cys, acetamidomethyl (Acm) thioether; Asn and Gln, trityl (Trt) amide; Ser, Thr and Tyr, tert-butyl (tBu) ether, and Lys, tert-butyloxycarbonyl (Boc) carbamate. Once chain assembly was completed, cyclization of *SoCCAPs* was performed by Tl(CF₃COO)₃ oxidation, as previously described (Chatenet et al., 2004). Peptides were deprotected and cleaved from the resin using TFA as previously described (Chatenet et al., 2006; Labarrère et al., 2003). Crude peptides were purified by reversed-phase HPLC (RP-HPLC) on a Vydac 218TP1022 C₁₈ column (2.2 x 25 cm; Grace Discovery Sciences Alltech, Templemars, France) using a linear gradient (10-50% over 50 min) of ACN/TFA (99.9:0.1, v/v) at a flow rate of 10 ml/min. Peptides were analyzed by RP-HPLC on a Vydac 218TP54 C₁₈ column (0.46 x 25 cm; Grace Discovery Sciences Alltech) using a linear gradient (10-60% over 25 min) of ACN/TFA (99.9:0.1, v/v) at a flow rate of 1 ml/min. The purity of all peptides was higher than 99.9%. The peptides were characterized by MALDI-TOF mass spectrometry on a Voyager DE-PRO (AB Sciex, Les Ulis, France) in the reflector mode, with CHCA as a matrix.

2.7 NMR and structure determination

2.7.1 NMR measurements

The nuclear magnetic resonance (NMR) samples containing 1-3 mM of peptides *SoCCAP1*, *SoCCAP2* and *SoCCAP3* were dissolved in water or in the presence of SDS micelles (150-200 mM) in a 5.1 - 5.7 pH range. All spectra were recorded on a Bruker Avance 500 spectrometer equipped with a 5-mm TCI cryoprobe (¹H, ¹³C, ¹⁵N). Homonuclear 2-D spectra DQF-COSY, TOCSY and ROESY or NOESY were typically recorded using standard Bruker

sequences in the phase-sensitive mode using the States-TPPI method. NOESY or ROESY spectra were acquired with 8 scans, 8 spectra were summed, leading to less t1 noise as recently reported (Mo et al., 2017). Typical spectra were acquired using matrices of 4,096 x 320-600 zero filled in F1 to 2K x 1K after apodization with shifted sine-square multiplication in both domains. Spectra were processed with Topspin software (Bruker) and analyzed with NMRview (Johnson, 2004).

2.7.2 Structure calculations

¹H chemical shifts were assigned according to the classical sequential assignment procedure. NOE cross-peaks were integrated and assigned in the NMRView software program (Johnson, 2004). The NOE peak volumes between methylene pair protons were used as 1.8-Å references. The lower bound for all restraints was fixed at 1.8 Å, and upper bounds at 2.7, 3.3 and 5.0 Å for strong, medium and weak correlations, respectively. Structure calculations were performed with AMBER 17 (Case et al., 2005) in two stages: cooking and simulated annealing in explicit solvent. The cooking stage was performed at 1,000 K to generate 100 initial random structures. Simulated annealing calculations were carried out during 20 ps (20,000 steps, 1 fs long). First, the temperature was risen quickly and was maintained at 1,000 K for the first 5,000 steps, then the system was cooled gradually from 1,000 K to 100 K from step 5,001 to 18,000, and finally the temperature was brought to 0 K during the 2,000 remaining steps. For the first 3,000 steps, the force constant of the distance restraints was increased gradually from 2.0 kcal.mol⁻¹.Å to 20 kcal.mol⁻¹.Å. For the rest of the simulation (step 3,001 to 20,000), the force constant was kept at 20 kcal.mol⁻¹.Å. The 15 lowest energy structures with no violations > 0.3 Å were considered as representative of the compound structure. Representation and quantitative analysis were carried out using MOLMOL (Koradi et al., 1996) or YASARA (Krieger et al., 2002).

2.8 Myotropic bioassay

The myotropic bioassay was performed using different contractile organs involved in egg-laying: MNGs, distal oviduct, proximal oviduct and ovarian stroma. Each organ was suspended on a dynamometer (Dynamometer UF1, Pioden controls LTD) in a muscle chamber, with a nylon thread (0.12-mm diameter). The signal was amplified by an amplifier (SGA 920201-01, Bionic instrument) and contractions were displayed on a printer (L200E, Linseis) or with Seriadinoplotter_1.1. This second imaging method is a homemade digital voltmeter based on Arduino technology (<https://www.arduino.cc>) coupled to the Qt application programming interface (<https://www.qt.io>). The muscle chamber was perfused at a flow rate of 0.5 mL.min⁻¹ with perfusion solution and maintained at 18 °C. Increasing concentrations of synthetic peptides were injected in the perfusing flow using a three-way valve to avoid mechanical stress. The flow of the samples into the muscle chamber was traced by adding phenol red.

3. Results

3.1 Expression patterns of *SoCCAPs* and *SoCCAP GPCR*

Expression patterns revealed that *SoCCAP* transcripts were expressed in the three main parts of the CNS: the optic lobes (OL), the supraesophageal mass (SupEM), and the subesophageal mass (SubEM) (Figure 2A). High levels of overexpression were observed in the SubEM, which is the part of the CNS that innervates viscera and the genital apparatus; it is connected to the only neurohemal area described in cuttlefish so far.

Expression of the *SoCCAP* receptor identified from the annotated *S. officinalis* transcriptome was mainly restricted to the MNGs and OvG, the accessory sex glands involved in egg-

capsule secretion. A very low expression level was also observed in the CNS, the posterior salivary glands, and the ovary (Figure 2B).

3.2 Transmembrane domains of CCAP GPCRs

Sequence alignment of *S. officinalis*, *Loligo pealei*, *Octopus bimaculoides* and *Apis mellifera* GPCRs allowed us to predict transmembrane domains using HMMTOP, TMHMM and I-TASSER, according to Garcia et al. (2015) (Figure 3). The two *L. pealei* Lp1 and Lp2 isoforms showed a high level of conservation with the GPCR identified in *S. officinalis*. The seven transmembrane domains were quite similarly organized in these two cephalopod decapod species, and so were amino acid sequences. For *O. bimaculoides* GPCR, only four or five transmembrane domains (depending of the web tools) were predicted. Sequence alignment revealed that the N-terminal sequence was truncated: it lacked the first and second predicted transmembrane domains, as well as a part of the third one.

3.3 Immunocytochemistry

The specificity of affinity purified polyclonal antibodies raised against SoCCAP1 was improved by using antibodies preabsorbed with antigen (not shown) or by omitting primary antibodies (Figures 4B-4D).

In the genital tract of egg-laying females (figure 4), immunostained nerve endings were observed in OvG blades and at the level of the distal end of the gland. Intense staining was also observed in the distal end surrounding the distal oviduct (Figure 4A-B). This particular staining did not correspond to cell bodies, so it probably enhanced large fiber bundles. In addition, similar immunostaining was observed in the distal end of the MNGs associated to the secretory duct (Figure 4C-D). Investigations at the level of the ovarian stroma did not reveal any immunostaining.

Tissue mapping was performed in the CNS (Figure 5A) and the genital tract of egg-laying females. Neurons and nerve fibers were stained in the posterior part of the paleovisceral lobe of the SubEM (Figure 5B). Immunostained neurons were observed in the median and anterior basal lobes of the SupEM (Figure 5C and 5D). Immunostained neurons and nerve fibers were also observed in the medulla of the OL.

3.4 Neuropeptides localization by mass spectrometry

Immunocytochemistry detection of SoCCAPs in the nerve endings of the distal area of MNGs and in the OvG motivated further investigations by mass spectrometry focused on the immunostained areas. The MS/MS spectrum of SoCCAP1 is presented in Figure 6. In addition, SoCCAPs were detected in the whole oviduct, together with cryptic peptides such as pQPQENTFQMKPSESDILNMKIRHLI, LFDEENDFKLVASDSIQPMEQETAID and AVQRQPTANDFSNEELASLPD (Figure 7A and B). A truncated form, PQQENTFQMKPSESDILNMKI, was also detected only in the distal end of the oviduct.

3.5 NMR assays

SoCCAP1, SoCCAP2, and SoCCAP3 ¹H NMR spectra were performed in water and in the presence of SDS micelles. For each SoCCAP, the greatest number of constraints was obtained in the presence of SDS micelles as compared to water. The NOE connectivity diagrams of the three SoCCAPs in water provided only sequential information, with $d\alpha N(i, i+1)$, $d\beta N(i, i+1)$ and $dNN(i, i+1)$ connectivities. In the presence of SDS micelles, while SoCCAP3 showed only a few additional cross-peaks, SoCCAP1 and SoCCAP2 NOE diagrams displayed several two-medium-range connectivities, *i.e.* five $d\alpha N(i, i+2)$ for SoCCAP2, and six $d\alpha N(i, i+2)$, four $dNN(i, i+2)$, and four $d\alpha N(i, i+3)$ for SoCCAP1. As the greatest amount of spatial

information was obtained for *SoCCAP2*, we decided to focus on this peptide to further study its structure in the presence of SDS micelles.

The ^1H chemical shifts of *SoCCAP1* in the presence of SDS micelles are given in Supplemental Table 1. In the final run, *SoCCAP1* structures were calculated using 81 inter-residue constraints. The 20 lowest energy structures without distance violation superior to 0.3 Å, out of the 100 structures calculated with AMBER, are presented in Figure 8A, and detailed lowest energy structure is shown in Figure 8B. These *SoCCAP1* structures displayed disordered N-terminal and C-terminal domains, and a well-defined cycle encompassing all the amino acids between cysteine residues 3 and 9. These two cysteine residues formed the disulfide bond conserved in CCAPs. The calculated rmsd for these 20 structures was 0.179 Å when considering the backbone and the disulfide bond, and 0.212 Å when considering all the heavy atoms between Cys³ and Cys⁹. Inside the stable Cys³-Cys⁹ cycle, two hydrogen bonds were defined between CO of Asn⁴ and NH of Gly⁷, and between CO of Ser⁵ and NH of Gly⁸, with ca. 2 Å between the two residues involved in each hydrogen bond. When considering these two hydrogen bonds in the 20 lowest energy structures, the distribution of the dihedral angles of residues *i*+1 and *i*+2 led to the identification of a type II β-turn for Asn⁴ - Gly⁷ and a type III' β-turn for Ser⁵ - Gly⁸ (Lewis et al., 1973).

3.6 Bioassays

Bioassays were carried out on the genital tract of egg-laying females, and also on the penis and deferent duct of mature males. The *SoCCAP1* peptide decreased the amplitude of MNG contractions, with a threshold of 10⁻⁹ M (Figure 9A). Similar activity levels were observed with *SoCCAP2* and *SoCCAP3*. *SoCCAP1* decreased the tonus of the proximal oviduct with a threshold at 10⁻⁹ M (Figure 9B). No effect was observed on the ovarian stroma of egg-laying females, the penis or the deferent duct of mature males, or in the genital tract of vitellogenic females. Based on the biological activities reported in arthropods, *SoCCAP1* was also tested on the vena cava of egg-laying females. An increase in the frequency and tonus of the vein contractions was observed, with a threshold of 10⁻⁸ M. All activities were dose-dependent, from 10⁻⁶ to 10⁻⁸ or 10⁻⁹ M (data not shown).

4 Discussion

In a previous paper, we showed that the *SoCCAP* precursor was expressed in different parts of the CNS and overexpressed in egg-laying females as compared to sexually mature males (Zatylny-Gaudin et al., 2016).

The present study addresses the putative involvement of *SoCCAPs* in the regulation of egg-laying through tissue expression patterns, tissue mapping of mature neuropeptides, identification and tissue mapping of receptor transcripts, and bioactivity of *SoCCAPs* on the genital tract. In addition, were performed structural investigations to determine *SoCCAP* structure in a medium that mimics a lipid membrane. The three mature neuropeptides detected in the OvG by mass spectrometry (Zatylny-Gaudin et al., 2016) suggest a role in the secretion of the inner oocyte capsule and / or in modulation of contractions of the distal oviduct which releases oocytes into the mantle cavity. Additional immunocytochemistry investigations carried out in the present study revealed the presence of *SoCCAPs* in OvG nerve endings and in the distal oviduct associated with this gland. New mass spectrometry analyses confirmed the previous results and demonstrated the concomitant occurrence of cryptic peptides.

Cryptic peptides or “cryptome” flanked by dibasic cleavage sites on protein precursors often have distinct biological properties from the peptides of their protein precursor. They appear to play a role in modulating biological processes such as angiogenesis, immune functions, cell growth, and offer new opportunities for protein-based therapy (Autelitano et al., 2006). Dylag et al. (2008) demonstrated the existence of a novel bioactive cryptic peptide within an already

known NPFF precursor. Bosso et al. (2017) described a cryptic host defense peptide in human 11-hydroxysteroid dehydrogenase-1 β -like. In this context, cryptic peptides cleaved from the *SoCCAP* protein precursor could have biological activities. They were detected in the oviduct, and possessed post-translational modifications such as an N-terminal pyroglutamate for one of them, or a conserved RHLI C-terminal sequence for two of them (Figure 7B).

Immunocytochemistry and mass spectrometry investigations on the distal end of the oviduct revealed the occurrence of immunostained nerve fibers and the presence of *SoCCAPs* and cryptic peptides. Tissue mapping of the neuropeptides and receptor associated to biological activity clearly established the involvement of *SoCCAPs* in the regulation of oocyte transport and also probably in the mechanical secretion of capsular products since the distal oviduct and the OvG are very closely associated.

Immunocytochemistry also revealed the presence of CCAP-like peptides in the nerve endings of the distal end of MNGs, according to mass spectrometry analyses. These large glands secrete the outer capsule of the egg and have a very similar histological organization to the OvG. A central axial channel collects the secretions released by microvilli lined with secretory cells. The secreting activity of these glands has to be synchronized with that of the OvG to allow egg-capsule formation. Mechanical secretion is therefore quite probably synchronized by the same families of regulators. Similarly to the OvG, MNGs expressed the *SoCCAP* receptor described above, and their contractions were modulated by *SoCCAPs*. Their effect on the OvG and MNGs suggests that they may be involved in regulating egg-capsule inner and/or outer layer secretion.

Interestingly, *SoCCAPs* had no myotropic activity in the ovarian stroma. This densely vascularized structure made of conjunctive tissue and muscle fibers is involved in ovulation, which in cuttlefish corresponds to the release of mature oocytes into the genital coelom. Thus, regulation by *SoCCAPs* seems to be restricted to specific reproductive functions.

Even if the effects of *SoCCAPs* observed in OvG and MNG decreased the tonus and the amplitude of contractions, it is important to keep in mind that we recorded the activity of a single isolated neuropeptide, a situation that never occurs in physiological conditions. Previous papers showed that APGWamide (Henry et al., 1997) as well as FMRFamide (Henry et al., 1999) induced strong modifications of the contractile activity of the oviduct. So we can assume that the contractile activity of the genital apparatus is regulated by a very complex cocktail of neuropeptides. This cocktail is probably able to cause successive contraction phases followed by rest periods to allow for a sustained activity throughout the several-day-long egg-laying period.

At the level of the CNS, in the SubEM and more particularly in the palaeovisceral lobe, clusters of immunostained neurons and fibers were observed. CCAP localization in this part of the CNS was previously confirmed by mass spectrometry, with the detection of the 3 *SoCCAPs* in SubEM (Zatylny-Gaudin et al., 2016). The presence of peptides potentially involved in reproduction in this part of the CNS is coherent because the palaeovisceral lobe is the lobe that innervates the genital tract and viscera. Moreover, this part of the CNS is coupled to the neurohemetic area of the vena cava, even if mass spectrometry analysis of haemolymph samples showed that *SoCCAPs* acted exclusively via nervous signals.

Immunostained neurons and fibers were also observed in the OL and SupEM. In the SupEM, only neurons were observed as a large cluster in the anterior part of the basal anterior lobe. This lobe is involved in the predatory behavior (Chichery and Chichery, 1987), and transcriptomic data indicated that the *SoCCAP* precursor was more expressed in the SupEM of egg-laying females. Therefore *SoCCAPs* may also be involved in predation, in order to build up reserves for spawning: our aquarium observations showed that female cuttlefish stopped feeding during spawning.

At the structural level, the presence of a disulfide bond in such a short primary sequence will constraint the cycle. However, small peptides (neuropeptides or antimicrobial peptides) are often unstructured in water but can acquire a well-defined tridimensional structure in a hydrophobic environment such as SDS micelles. This medium mimics the lipid membrane and is assumed to induce structures close to the receptor-bound peptide conformations. Accordingly to such a scheme, NMR analyses in water did not yield much data about the three-dimensional conformation of *SoCCAPs*. The three *SoCCAPs* displayed only sequential constraints, in agreement with an unstable structure of these peptides in aqueous medium. In contrast, in the presence of SDS micelles, more medium-range connectivity was observed in NOESY spectra. Nevertheless, the extent of medium-range connectivity was also dependent on the *SoCCAP* studied; this suggests a role of the C-terminal domain, which is specific to each *SoCCAP*, in 3D structure stabilization. The structure of *SoCCAP1* was solved in the presence of SDS micelles. We determined the presence of two types of β -turns inside the stable cyclic structure.

CCAP structures have only been described in a few arthropod and mollusk species, including an insect - the fruit fly *D. melanogaster* -, a crustacean - the crab *C. maenas* -, and a gastropod mollusk - the marine cone snail *Conus villepini* - (Jackson et al., 2009; Miloslavina et al., 2010; Nagata and Tanokura, 2005). In *D. melanogaster*, NOE analysis of CCAP in water showed that most interactions were sequential, with only few medium-range and long-range connectivities (Jackson et al., 2009). The disulfide bond obviously confers all reported CCAPs a cyclic structure given by the two cysteine residues. In the marine cone snail *C. villepini*, the N-terminal and C-terminal domains have been described as more flexible (Miloslavina et al., 2010). In *C. maenas* and *D. melanogaster*, the CCAP sequence is shorter and ends by Cys⁹, which is involved in the disulfide bond (Jackson et al., 2009; Nagata and Tanokura, 2005). The N-terminal end presents a high degree of flexibility. The well-defined cycle between the cysteine residues implied in the conserved disulfide bond could represent a conserved structure of CCAPs in protostomes, with the presence of flanking N-terminal and C-terminal disordered domains, when they exist in the sequence.

While the presence of a β -turn inside the stable cyclic structure appears to be common in protostomes, the β -turn type varies among species. In the crab *C. maenas*, a type-IV β -turn was described between residues Ala⁵ and Gly⁸, and in the marine cone snail *C. villepini* a type-I β -turn was described between residues Asn⁴ and Gly⁷ (Jackson et al., 2009; Miloslavina et al., 2010).

In cephalopods, the primary sequence of CCAPs is highly conserved among species. For example, the primary sequences of *S. officinalis* and *L. pealei* CCAPs are fully conserved (Figure 10). This homology will have to be confirmed in cephalopod decapods once novel transcriptomes or genomes are available. The high level of sequence conservation in regulatory peptides is often associated to regulation of important functions. In insects, e.g. *Rhodnius prolixus*, CCAP is essential for ecdysis (Lee et al., 2013). The first indication of CCAP involvement in ecdysis was decreased staining intensity in neurons containing CCAP immediately after ecdysis, suggesting CCAP release. CCAP also has a role in circular activity by controlling the heart rate. In *L. migratoria*, CCAP increased the basal tonus and the frequency and amplitude of phasic contractions (Donini et al., 2001). Unlike in *S. officinalis*, no CCAP-like immunoreactive structures were observed in the nerves innervating the oviduct, suggesting that CCAPs probably acted as neurohormones. Still in *L. migratoria*, CCAP-like immunostained cells were discovered in the fat body associated with the oviducts that represents a potential source of CCAP, along the transverse nerve and perivisceral organs. In the mosquito *A. gambiae*, CCAP increased the contraction rate of the auxiliary hearts, the organ that controls hemolymph circulation in the antennae (Suggs et al., 2016). In *S.*

officinalis CCAPs increased the vena cava tonus in a dose-dependent manner; this demonstrates their involvement in the regulation of hemolymph circulation (data not shown). In *R. prolixus*, the CCAP receptor (RhoCCAPR) is expressed in the female and male reproductive systems and salivary glands (Lee et al., 2013). In *S. officinalis*, expression of the only SoCCAP receptor identified so far was restricted to the OvG and MNGs, and was not recovered in the salivary glands of either sex. CCAP GPCR organization showed a high level of conservation between cephalopods and arthropods, with very similar transmembrane domains.

Finally, in arthropods and cephalopods, conservation of neuropeptide and GPCR structures appears to be associated to conservation of regulated functions, e.g. hemolymph circulation and reproduction (gamete release), except ecdysis that is of course restricted to arthropods.

This study shows that CCAPs expressed in cuttlefish are certainly involved in oocyte transport and egg-capsule secretion. They probably also play a role in the release of oocytes into the mantle cavity near the secretory orifices of the MNGs. Regarding expression data, the tissue mapping of neuropeptides as well as the distribution of receptors, we can speculate that CCAPs are one of the main neuropeptide family involved in egg-laying regulation as FMRFamide, APGWamide and sepiatocin.

Further cellular investigations will have to be performed to determine their putative involvement in the regulation of egg-capsule synthesis during vitellogenesis.

Acknowledgments

We thank Jean-Luc Blaie and Maxime Marie, captains of the professional fishing boats “Père Daniel” and “Bip-Bip”, and their crews for their valuable help in providing cuttlefish. We thank Beatrice Adeline for technical support in histological analysis, and Christophe Roger for technical support in the construction of specific equipments. We thank Drs Baptiste Legrand and Matthieu Simon for their help with the AMBER software program. This work was financed by the ANR "NEMO" and the Conseil regional of BASSE-NORMANDIE.

References

- Adams, M.D., Celniker, S.E., Holt, R.A., Evans, C.A., Gocayne, J.D., Amanatides, P.G., Scherer, S.E., Li, P.W., Hoskins, R.A., Galle, R.F., George, R.A., Lewis, S.E., Richards, S., Ashburner, M., Henderson, S.N., Sutton, G.G., Wortman, J.R., Yandell, M.D., Zhang, Q., Chen, L.X., Brandon, R.C., Rogers, Y.C., Blazej, R.G., Champe, M., Pfeiffer, B.D., Wan, K.H., Doyle, C., Baxter, E.G., Helt, G., Nelson, C.R., Miklos, G.L.G., Abril, J.F., Agbayani, A., An, H., Andrews-pfannkoch, C., Baldwin, D., Ballew, R.M., Basu, A., Baxendale, J., Bayraktaroglu, L., Beasley, E.M., Beeson, K.Y., Benos, P. V, Berman, B.P., Bhandari, D., Bolshakov, S., Borkova, D., Botchan, M.R., Bouck, J., Brokstein, P., Brottier, P., Burtis, K.C., Busam, D.A., Butler, H., Cadieu, E., Chandra, I., Cherry, J.M., Cawley, S., Dahlke, C., Davenport, L.B., Davies, P., Pablos, B. De, Delcher, A., Deng, Z., Mays, A.D., Dew, I., Dietz, S.M., Dodson, K., Doup, L.E., Downes, M., Dugan-rocha, S., Dunkov, B.C., Dunn, P., Durbin, K.J., Evangelista, C.C., Ferraz, C., Ferriera, S., Fleischmann, W., Fosler, C., Gabrielian, A.E., Garg, N.S., Gelbart, W.M., Glasser, K., Glodek, A., Gong, F., Gorrell, J.H., Gu, Z., Guan, P., Harris, M., Harris, N.L., Harvey, D., Heiman, T.J., Hernandez, J.R., Houck, J., Hostin, D., Houston, K.A., Howland, T.J., Wei, M., Ibegwam, C., Jalali, M., Kalush, F., Karpen, G.H., Ke, Z., Kennison, J.A., Ketchum, K.A., Kimmel, B.E., Kodira, C.D., Kraft, C., Kravitz, S., Kulp, D., Lai, Z., Lasko, P., Lei, Y., Levitsky, A.A., Li, J., Li, Z., Liang, Y., Lin, X., Liu, X., Mattei, B., Mcintosh, T.C., Mcleod, M.P., Mcpherson, D., Merkulov, G., Milshina,

- N. V., Mobarry, C., Morris, J., Moshrefi, A., Mount, S.M., Moy, M., Murphy, B., Murphy, L., Muzny, D.M., Nelson, D.L., Nelson, D.R., Nelson, K.A., Nixon, K., Nusskern, D.R., Pacleb, J.M., Palazzolo, M., Pittman, G.S., Pan, S., Pollard, J., Puri, V., Reese, M.G., Reinert, K., Remington, K., Saunders, R.D.C., Scheeler, F., Shen, H., Shue, B.C., Side, I., Simpson, M., Skupski, M.P., Smith, T., Spier, E., Spradling, A.C., Stapleton, M., Strong, R., Sun, E., Svirskas, R., Tector, C., Turner, R., Venter, E., Wang, A.H., Wang, X., Wang, Z., Wassarman, D.A., Weinstock, G.M., Weissenbach, J., Williams, S.M., Woodage, T., Worley, K.C., Wu, D., Yang, S., Yao, Q.A., Ye, J., Yeh, R., Zaveri, J.S., Zhan, M., Zhang, G., Zhao, Q., Zheng, L., Zheng, X.H., Zhong, F.N., Zhong, W., Zhou, X., Zhu, S., Zhu, X., Smith, H.O., Gibbs, R.A., Myers, E.W., Rubin, G.M., Venter, J.C., 2000. The Genome Sequence of *Drosophila melanogaster* 287, 2185–2195.
- Ahn, S.J., Martin, R., Rao, S., Choi, M.Y., 2017. Neuropeptides predicted from the transcriptome analysis of the gray garden slug *Deroceras reticulatum*. *Peptides* 93, 51–65.
- Arch, S., 1972. Biosynthesis of the egg-laying hormone (ELH) in the bag cell neurons of *Aplysia californica*. *J. Gen. Physiol.* 60, 102–119.
- Autelitano, D.J., Rajic, A., Smith, A.I., Berndt, M.C., Ilag, L.L., Vadas, M., 2006. The cryptome: a subset of the proteome, comprising cryptic peptides with distinct bioactivities. *Drug Discov. Today* 11, 306–314.
- Baker, J.D., McNabb, S.L., Truman, J.W., 1999. The hormonal coordination of behavior and physiology at adult ecdysis in *Drosophila melanogaster*. *J. Exp. Biol.* 202, 3037–3048.
- Bernay, B., Baudy-Floc'h, M., Zanuttini, B., Gagnon, J., Henry, J., 2005. Identification of SepCRP analogues in the cuttlefish *Sepia officinalis*: A novel family of ovarian regulatory peptides. *Biochem. Biophys. Res. Commun.* 338, 1037–1047.
- Bernay, B., Baudy-Floc'h, M., Zanuttini, B., Zatylny, C., Pouvreau, S., Henry, J., 2006. Ovarian and sperm regulatory peptides regulate ovulation in the oyster *Crassostrea gigas*. *Mol. Reprod. Dev.* 73, 607–616.
- Bernay, B., Gagnon, J., Henry, J., 2004. Egg capsule secretion in invertebrates: a new ovarian regulatory peptide identified by mass spectrometry comparative screening in *Sepia officinalis*. *Biochem. Biophys. Res. Commun.* 314, 215–222.
- Case, D.A., Cheatham III, T.E., Darden, T., Gohlke, H., Luo, R., Merz JR., K.M., Onufriev, A., Simmerling, C., Wang, B., Woods, R.J., 2005. The Amber Biomolecular Simulation Programs. *J. Comput. Chem.* 26, 1668–1688.
- Chatenet, D., Dubessy, C., Boularan, C., Scalbert, E., Pfeiffer, B., Renard, P., Lihmann, I., Pacaud, P., Tonon, M.C., Vaudry, H., Leprince, J., 2006. Structure-activity relationships of a novel series of urotensin II analogues: Identification of a urotensin II antagonist. *J. Med. Chem.* 49, 7234–7238.
- Chatenet, D., Dubessy, C., Leprince, J., Boularan, C., Carlier, L., Ségalas-Milazzo, I., Guilhaudis, L., Oulyadi, H., Davoust, D., Scalbert, E., Pfeiffer, B., Renard, P., Tonon, M.C., Lihmann, I., Pacaud, P., Vaudry, H., 2004. Structure-activity relationships and structural conformation of a novel urotensin II-related peptide. *Peptides* 25, 1819–1830.
- Chichery, M.P., Chichery, R., 1987. The Anterior Basal Lobe and Control of Prey-Capture in the Cuttlefish (*Sepia officinalis*). *Physiol. Behav.* 40, 329–336.
- Chiu, A.Y., Hunkapiller, M.W., Heller, E., Stuart, D.K., Hood, L.E., Strumwasser, F., 1979. Purification and primary structure of the neuropeptide egg-laying hormone of *Aplysia*

- californica*. Proc. Natl. Acad. Sci. U. S. A. 76, 6656–6660.
- Chiu, A.Y., Strumwasser, F., 1981. An Immunohistochemical Study of the Neuropeptidergic Bag Cells of *Aplysia*. J. Neurosci. 1, 812–826.
- Christie, A.E., Roncalli, V., Cieslak, M.C., Pascual, M.G., Yu, A., Lameyer, T.J., Stanhope, M.E., Dickinson, P.S., 2017. Prediction of a neuropeptidome for the eyestalk ganglia of the lobster *Homarus americanus* using a tissue-specific de novo assembled transcriptome. Gen. Comp. Endocrinol. 243, 96–119.
- Chung, J.S., Wilcockson, D.C., Zmora, N., Zohar, Y., Dirksen, H., Webster, S.G., 2006. Identification and developmental expression of mRNAs encoding crustacean cardioactive peptide (CCAP) in decapod crustaceans. J. Exp. Biol. 209, 3862–3872.
- Cornet, V., Henry, J., Goux, D., Duval, E., Bernay, B., Le Corguillé, G., Corre, E., Zatylny-Gaudin, C., 2015. How Egg Case Proteins Can Protect Cuttlefish Offspring? PLoS One 10, e0132836.
- da Silva, R., Lange, A.B., 2006. The association of crustacean cardioactive peptide with the spermatheca of the African migratory locust, *Locusta migratoria*. J. Insect Physiol. 52, 399–409.
- Donini, A., Agricola, H.J., Lange, A.B., 2001. Crustacean cardioactive peptide is a modulator of oviduct contractions in *Locusta migratoria*. J. Insect Physiol. 47, 277–285.
- Dulcis, D., Levine, R.B., 2003. Innervation of the heart of the adult fruit fly, *Drosophila melanogaster*. J. Comp. Neurol. 465, 560–578.
- Dulcis, D., Levine, R.B., Ewer, J., 2005. Role of the neuropeptide CCAP in *Drosophila* cardiac function. J. Neurobiol. 64, 259–274.
- Dylag, T., Pachuta, A., Raoof, H., Kotlinska, J., Silberring, J., 2008. A novel cryptic peptide derived from the rat neuropeptide FF precursor reverses antinociception and conditioned place preference induced by morphine. Peptides 29, 473–478.
- Ebberink, R.H., van Loenhout, H., Geraerts, W.P., Joosse, J., 1985. Purification and amino acid sequence of the ovulation neurohormone of *Lymnaea stagnalis*. Proc. Natl. Acad. Sci. U. S. A. 82, 7767–71.
- Enault, J., Zatylny-Gaudin, C., Bernay, B., Lefranc, B., Leprince, J., Baudy-Floc'h, M., Henry, J., 2012. A complex set of sex pheromones identified in the cuttlefish *Sepia officinalis*. PLoS One 7, e46531.
- Estévez-Lao, T.Y., Boyce, D.S., Honegger, H.-W., Hillyer, J.F., 2013. Cardioacceleratory function of the neurohormone CCAP in the mosquito *Anopheles gambiae*. J. Exp. Biol. 216, 601–13.
- Furuya, K., Liao, S., Reynolds, S.E., Ota, R.B., Hackett, M., Schooley, D. a, 1993. Isolation and Identification of a Cardioactive Peptide From *Tenebrio Molitor* and *Spodoptera Eridania* 374, 1065–1074.
- Garcia, V.J., Daur, N., Temporal, S., Schulz, D.J., Bucher, D., 2015. Neuropeptide Receptor Transcript Expression Levels and Magnitude of Ionic Current Responses Show Cell Type-Specific Differences in a Small Motor Circuit. J. Neurosci. 35, 6786–6800.
- Geraerts, W.P.M., Cheeseman, P., Ebberink, R.H.M., Nuyt, K., Hogenes, T.M., 1983. Partial purification and characterization of the ovulation hormone of the freshwater pulmonate snail *Lymnaea stagnalis*. Gen. Comp. Endocrinol. 51, 471–476.
- Gonçalves, R.A., Aragão, C., Frias, P.A., Sykes, A. V., 2012. The use of different

- anaesthetics as welfare promoters during short-term human manipulation of European cuttlefish (*Sepia officinalis*) juveniles. *Aquaculture* 370–371, 130–135.
- Henry, J., Cornet, V., Bernay, B., Zatylny-Gaudin, C., 2013. Identification and expression of two oxytocin/vasopressin-related peptides in the cuttlefish *Sepia officinalis*. *Peptides* 46, 159–66.
- Henry, J., Favrel, P., Boucaud-Camou, E., 1997. Isolation and identification of a novel Ala-Pro-Gly-Trp-amide-related peptide inhibiting the motility of the mature oviduct in the cuttlefish, *Sepia officinalis*. *Peptides* 18, 1469–1474.
- Henry, J., Zatylny, C., Boucaud-Camou, E., 1999. Peptidergic control of egg-laying in the cephalopod *Sepia officinalis*: Involvement of FMRFamide and FMRFamide-related peptides. *Peptides* 20, 1061–1070.
- Honegger, H.W., Market, D., Pierce, L. a., Dewey, E.M., Kostron, B., Wilson, M., Choi, D., Klukas, K. a., Mesce, K. a., 2002. Cellular localization of bursicon using antisera against partial peptide sequences of this insect cuticle-sclerotizing neurohormone. *J. Comp. Neurol.* 452, 163–177.
- In, V. Van, Ntalamagka, N., Connor, W.O., Wang, T., Powell, D., Cummins, S.F., Elizur, A., 2016. Peptides Reproductive neuropeptides that stimulate spawning in the Sydney Rock Oyster (*Saccostrea glomerata*). *Peptides* 82, 109–119.
- Jackson, G.E., Mabula, A.N., Stone, S.R., Gäde, G., Kövér, K.E., Szilágyi, L., van der Spoel, D., 2009. Solution conformations of an insect neuropeptide: Crustacean cardioactive peptide (CCAP). *Peptides* 30, 557–564.
- Johnson, B.A., 2004. Using NMRView to visualize and analyze the NMR spectra of macromolecules. *Methods Mol. Biol.* 278, 313–352.
- Koradi, R., Billeter, M., Wüthrich, K., 1996. MOLMOL: A program for display and analysis of macromolecular structures. *J. Mol. Graph.* 14, 51–55.
- Krieger, E., Koraimann, G., Vriend, G., 2002. Increasing the precision of comparative models with YASARA NOVA - A self-parameterizing force field. *Proteins Struct. Funct. Genet.* 47, 393–402.
- Labarrère, P., Chatenet, D., Leprince, J., Marionneau, C., Loirand, G., Tonon, M.-C., Dubessy, C., Scalbert, E., Pfeiffer, B., Renard, P., Calas, B., Pacaud, P., Vaudry, H., 2003. Structure-activity relationships of human urotensin II and related analogues on rat aortic ring contraction. *J. Enzyme Inhib. Med. Chem.* 18, 77–88.
- Lee, D., Orchard, I., Lange, A.B., 2013. Evidence for a conserved CCAP-signaling pathway controlling ecdysis in a hemimetabolous insect, *Rhodnius prolixus*. *Front. Neurosci.* 7, 1–9.
- Lehman, H.K., Murguic, C.M., Miller, T. a., Lee, T.D., Hildebrand, J.G., 1993. Crustacean cardioactive peptide in the sphinx moth, *Manduca sexta*. *Peptides*.
- Lewis, P.N., Momany, F.A., Scheraga, H.A., 1973. Chain reversals in proteins. *BBA - Protein Struct.* 303, 211–229.
- Loi, P.K., Emmal, S. a, Park, Y., Tublitz, N.J., 2001. Identification, sequence and expression of a crustacean cardioactive peptide (CCAP) gene in the moth *Manduca sexta*. *J. Exp. Biol.* 204, 2803–16.
- McGaw, I.J., Wilkens, J.L., McMahon, B.R., Airriess, C.N., 1995. Crustacean cardioexcitatory peptides may inhibit the heart in vivo. *J. Exp. Biol.* 198, 2547–2550.

- Miloslavina, A., Ebert, C., Tietze, D., Ohlenschläger, O., Englert, C., Görlach, M., Imhof, D., 2010. An unusual peptide from *Conus vilpepinii*: Synthesis, solution structure, and cardioactivity. *Peptides* 31, 1292–1300.
- Mo, H., Harwood, J.S., Yang, D., Post, C.B., 2017. A simple method for NMR t1 noise suppression. *J. Magn. Reson.* 276, 43–50.
- Nagata, K., Tanokura, M., 2005. Cardioacceleratory peptide (CCAP) of the fruit fly *Drosophila melanogaster*: solution structure analysis and docking simulation to the receptor CG6111. *Pept. Sci.* 41, 441–444.
- Quan, F.B., Dubessy, C., Galant, S., Kenigfest, N.B., Djenoune, L., Leprince, J., Wyart, C., Lihmann, I., Tostivint, H., 2015. Comparative distribution and in vitro activities of the urotensin II-related peptides URP1 and URP2 in zebrafish: Evidence for their colocalization in spinal cerebrospinal fluid-contacting neurons. *PLoS One* 10, 1–21.
- Stangier, J., Hilbich, C., Beyreuther, K., Keller, R., 1987. Unusual cardioactive peptide (CCAP) from pericardial organs of the shore crab *Carcinus maenas*. *Proc. Natl. Acad. Sci.* 84, 575–579.
- Suggs, J.M., Jones, T.H., Murphree, S.C., Hillyer, J.F., 2016. CCAP and FMRamide-like peptides accelerate the contraction rate of the antennal accessory pulsatile organs (auxiliary hearts) of mosquitoes. *J. Exp. Biol.* 219, 2388–2395.
- Toullec, J., Corre, E., Mandon, P., Gonzalez-aravena, M., Ollivaux, C., Lee, C., 2017. Characterization of the neuropeptidome of a Southern Ocean decapod, the Antarctic shrimp *Chorismus antarcticus*: Focusing on a new decapod ITP-like peptide belonging to the CHH peptide family. *Gen. Comp. Endocrinol.* 252, 60–78.
- Toullec, J.Y., Corre, E., Bernay, B., Thorne, M. a. S., Cascella, K., Ollivaux, C., Henry, J., Clark, M.S., 2013. Transcriptome and Peptidome Characterisation of the Main Neuropeptides and Peptidic Hormones of a Euphausiid: The Ice Krill, *Euphausia crystallorophias*. *PLoS One* 8, e71609.
- Veenstra, J. a, 2010. Neurohormones and neuropeptides encoded by the genome of *Lottia gigantea*, with reference to other mollusks and insects. *Gen. Comp. Endocrinol.* 167, 86–103.
- Vreugdenhil, E., Geraerts, W.P.M., Jackson, J.F., Joosse, J., 1985. The molecular basis of the neuro-endocrine control of egg-laying behaviour in *Lymnaea*. *Peptides* 6, 465–470.
- York, P.S., Cummins, S.F., Degnan, S.M., Woodcroft, B.J., Degnan, B.M., 2012. Marked changes in neuropeptide expression accompany broadcast spawnings in the gastropod *Haliotis asinina*. *Front. Zool.* 9, 9.
- Zatylny-Gaudin, C., Cornet, V., Leduc, A., Zanuttini, B., Corre, E., Le Corguillé, G., Bernay, B., Garderes, J., Kraut, A., Couté, Y., Henry, J., 2016. Neuropeptidome of the Cephalopod *Sepia officinalis*: Identification, Tissue Mapping, and Expression Pattern of Neuropeptides and Neurohormones during Egg Laying. *J. Proteome Res.* 15, 48–67.
- Zatylny, C., Gagnon, J., Boucaud-Camou, E., Henry, J., 2000a. ILME: A Waterborne Pheromonal Peptide Released by the Eggs of *Sepia officinalis*. *Biochem. Biophys. Res. Commun.* 275, 217–222.
- Zatylny, C., Gagnon, J., Boucaud-Camou, E., Henry, J., 2000b. The SepOvotropein: A New Ovarian Peptide Regulating Oocyte Transport in *Sepia officinalis*. *Biochem. Biophys. Res. Commun.* 276, 1013–1018.

Figure 1: (A) Sequence alignment of CCAP protein precursors of (Ac) *Aplysia californica* (LOC101863916), (Dr) *Deroceras reticulatum* (ARS01357.1) (ARS01358.1), (So) *Sepia officinalis*, (Cg) *Crassostrea gigas* (XP_011446187.2), and (Cm) *Carcinus maenas* (ABB46291.1). Signal peptides are highlighted in yellow, and predicted neuropeptides in red. (B) Sequence alignment of CCAPs from *Sepia officinalis*, *Deroceras reticulatum*, *Aplysia californica*, *Carcinus maenas*, and *Crassostrea gigas*. C-terminal amidations are indicated by the letter a.

Figure 2: Tissue expression patterns: dark blue bars for SoCCAPs (A), light blue bars for SoCCAP GPCR (B) in egg-laying females (expressed in FPKM). Red bars for elongation protein 3 as a reference gene. ANG: Accessory nidamental gland; MNGs: Main nidamental glands; OvG: Oviduct gland; PSG: Posterior salivary gland; OL: Optic lobe; SupEM: Supraesophageal Mass; SubEM: Subesophageal Mass; OG: Optic gland. Organs belonging to the genital apparatus are in bold orange; the CNS is in bold green.

Figure 3: Multiple sequence alignment of the cuttlefish CCAP receptor sequence with the receptor sequences of *Octopus bimaculoides* (XP_014778737.1) (Ob), *Loligo pealei* (Lp) (<http://ivory.idyll.org/blog/2014-loligo-transcriptome-data.html>), and *Apis mellifera* (XP_001122652.2) (Am). Transmembrane domains are highlighted in red.

Figure 4: (A): Longitudinal section of the CNS of *Sepia officinalis* egg-laying females. Lobes belonging to the SupEM: mbL: median basal lobe; vL: vertical lobe; sFL: superior frontal lobe; iFL: inferior frontal lobe; abL: anterior basal lobe. Lobes belonging to the SubEM: pvL: palleo-visceral lobe; pL: pedal lobe; bL: brachial lobe. E: esophagus. Counter staining: Trichrome of Prenant-Grabe. (B): presence of SoCCAP immunostained neurons and fibers in the palleo-visceral lobe of the SubEM; (C): presence of SoCCAP immunostained neurons in the median basal lobe of the SupEM; (D): presence of SoCCAP immunostained neurons in the anterior basal lobe of the SupEM. Counterstaining: hematoxylin.

Figure 5: (A): Presence of immunostained fiber bundles in the distal end of the oviduct with SoCCAP antibodies, (B): Negative control without a primary antibody. (C): Presence of immunostained fiber bundles in the distal part of the MNG. (D): Negative control without a primary antibody. Scale bar: 50µm. Counterstaining: hematoxylin.

Figure 6: Off-line nLC-MALDI tandem MS analysis of the OvG: MS/MS spectrum of SoCCAP1 (VFCNSFGGCTNI).

Figure 7: Cryptic peptides cleaved from the SoCCAP protein precursor. (A): Off-line nLC-MALDI tandem MS analysis of the distal end of the oviduct. MS/MS spectrum of cryptic peptide 1 (m/z 2,979.7) predicted from the SoCCAP protein precursor. Immonium, a, b, y, and detected internal ions are indicated. (B): SoCCAP protein precursor: the predicted signal peptide is highlighted in yellow,

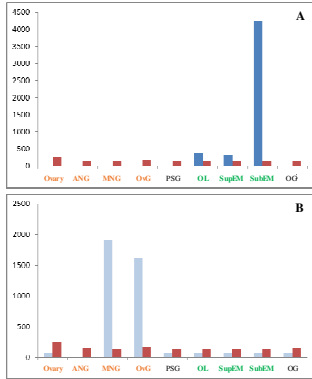
predicted convertase cleavage sites in red, N-terminal glutamine predicted to be converted into pyroglutamic acid in dark gray, cryptic peptides detected by mass spectrometry in light gray. Cryptic peptides are indicated in italics, *SoCCAPs* in bold, and conserved C-terminal sequences of cryptic peptides 1 and 5 are highlighted in green.

Figure 8: (A) Overlay of the 20 lowest energy structures with no violations $> 0.3 \text{ \AA}$ from the 100 structures calculated with AMBER software for neuropeptide *SoCCAP2* in SDS micelles. Overlay was performed using the backbone atoms of residues 3–8. (B) Detail of the lowest energy structure of *SoCCAP2* in SDS micelles displaying the hydrogen bonds between Asn4-Gly7 and Ser5-Gly8 (yellow dashes). N-term and C-term were omitted for clarity. The disulfide bridge is indicated in green.

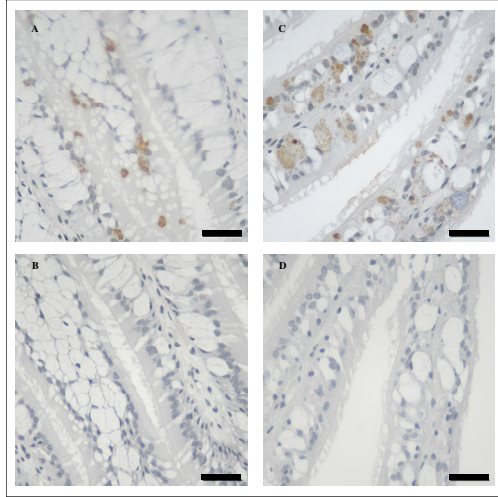
Figure 9: Dose-dependent myotropic effect of *SoCCAP1* applied to the MNGs (A) and distal oviduct (B) of egg-laying females.

Figure 10: Sequence alignment of the CCAP protein precursors of *Sepia officinalis* and *Loligo pealei*, two cephalopod decapods (<http://ivory.idyll.org/blog/2014-loligo-transcriptome-data.html>). The predicted neuropeptides highlighted in green are conserved in the two species. Signal peptides are highlighted in yellow, predicted dibasic cleavage sites in red, C-terminal conserved sequences of cryptic peptides in dark orange, the N-terminal pyroglutamic acid of cryptic peptide 1 detected in *Sepia officinalis* and predicted in *Loligo pealei* in blue.

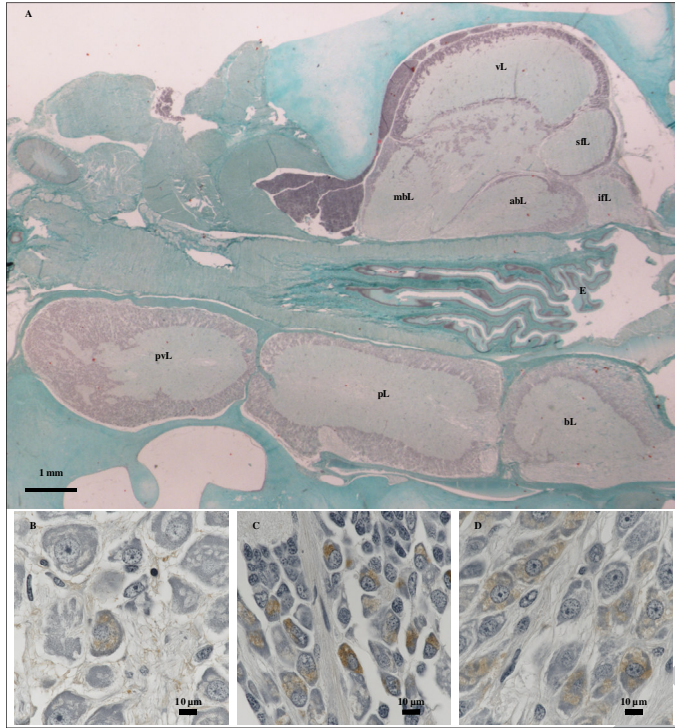
Table 1: Proton chemical shifts (ppm) of CCAP1 (1 mM) in 150 mM of SDS micelles at pH 5.7 at 303K.

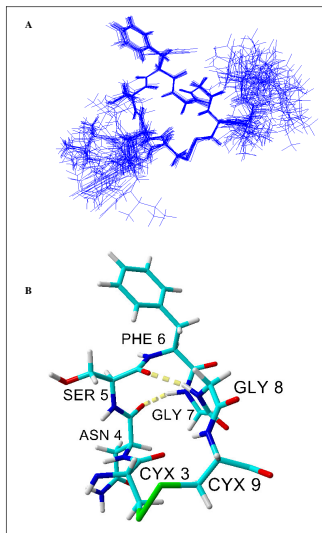


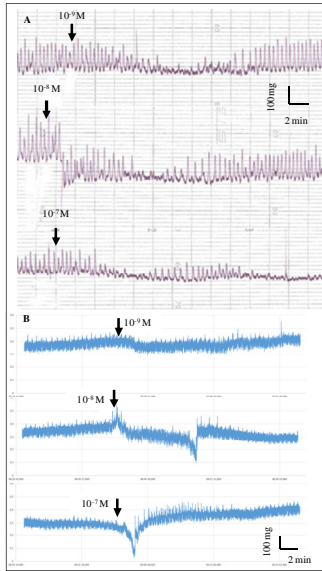
ACCEPTED MANUSCRIPT



ACCEPTED MANUSCRIPT







ACCEPTED MANUSCRIPT

```
Lp-CCAP MDSDEELSTGLLELYVYVLLDQTEFRVANSQPDIS - QMKPKSDNLSLLELLELLELAVGRQPTADATFDEELAPFPCQRFVNSFSGDQTN 54  
Ss-CCAP MDSFDEELSTGLLELYVYVLLDQTEFRVANSQPDIS - QMKPKSDNLSLLELLELLELAVGRQPTADATFDEELAPFPCQRFVNSFSGDQTN 54  
MQSgSSSLSTGLLELYVYVLLDQTEFRVANSQPDIS - QMKPKSDNLSLLELLELLELAVGRQPTADATFDEELAPFPCQRFVNSFSGDQTN 54  
Lp-CCAP RLFDIENDFKLVgDSLQPaEQETAIDKRVFCNSYGGCKSFKRV SANDzKkPmKkQRHLIRRLKkQP IKsRRVFCNSFGGQCN 180  
Ss-CCAP RLFDIENDFKLVgDSLQPaEQETAIDKRVFCNSYGGCKSFKRV SANDzKkPmKkQRHLIRRLKkQP IKsRRVFCNSFGGQCN 181
```

ACCEPTED MANUSCRIPT

Residue	H ^N	HA	HB2	HB3	HG2	HG3	HD1	HD2	Others
Val ¹	-	3.86	2.14		0.92	0.92			
Phe ²	8.41	4.66	3.17	3.24			7.30	7.30	HE1/2 HZ 7.18
Cys ³	8.13	4.55	3.09	3.09					
Asn ⁴	8.34	4.55	2.80	2.91					CONH ₂ 6.74/7.49
Ser ⁵	7.96	4.34	3.70	3.70					
Phe ⁶	8.03	4.56	3.00	3.20			7.25	7.25	HE1/2 HZ 7.18
Gly ⁷	8.14	3.87/4.0 4							
Gly ⁸	7.81	4.05/4.0 5							
Cys ⁹	8.37	4.69	3.11	3.24					
Thr ¹⁰	8.04	4.32	4.24		1.18				
Asn ¹¹	8.22	4.80	2.73	2.87					CONH ₂ 6.83/7.49
Ile ¹²	7.51	4.05	1.83		1.08/1.39	0.85	0.85		

- 1/ the first evidence of the involvement of crustacean cardio active peptides in the regulation of egg-laying in a cephalopod
- 2/ tissue mapping of neuropeptides performed both by immunochemistry and mass spectrometry
- 3/ expression pattern of both neuropeptides and GPCR
- 4/ functional characterization

ACCEPTED MANUSCRIPT